

Fully analytic implementation of density functional theory for efficient calculations on large molecules

Rajendra R. Zope*

Department of Chemistry, George Washington University, Washington DC, 20052, USA and

Department of Physics, University of Texas at El Paso, El Paso, Texas 79959, USA

Brett I. Dunlap[†]

³ *Code 6189, Theoretical Chemistry Section, US Naval Research Laboratory, Washington, DC 20375, USA*

(Dated: October 9, 2018)

Fullerene like cages and nanotubes of carbon and other inorganic materials are currently under intense study due to their possible technological applications. First principle simulations of these materials are computationally challenging due to large number of atoms. We have recently developed a fast, variational and fully analytic density functional theory (ADFT) based model that allows study of systems larger than those that can be studied using existing density functional models. Using polarized Gaussian basis sets (6-311G**) and ADFT, we optimize geometries of large fullerenes, fullerene-like cages and nanotubes of carbon, boron nitride, and aluminum nitride containing more than two thousand atoms. The calculation of C₂₁₆₀ using nearly 39000 orbital basis functions is the largest calculation on any isolated molecule reported to-date at this level of theory, and it includes full geometry optimization. The electronic structure related properties of the inorganic cages and other carbon fullerenes have been studied.

PACS numbers:

Keywords: boron nitride, nanotubes, fullerene

Computer simulations are playing increasingly important role in our understanding about materials. Generally, the choice of computational models that are employed in studying the properties of materials depend on the property of interest and the length scale or the size of the system[1]. The latter is the most important factor in the selection of appropriate level of theory. Our interest is in the electronic and structural properties of large carbon fullerenes and fullerene like cages of aluminum and boron nitride containing a few hundred atoms. At these sizes, the current toolbox of methods that are available include semiempirical quantum mechanical models such as ZINDO[2], PM3[3] methods or tight binding approaches[4]. More accurate description of electronic properties require use of more involved meth-

ods such as density functional (DF) based models[5, 6]. The traditional quantum chemical beyond Hartree-Fock methods or quantum Monte Carlo are, in general, more accurate than the DF models. However, they are suitable for systems with a few tens of atoms. At present, the applicability of DF models is restricted to two to three hundred atoms depending on the schemes used to approximate kinetic and exchange energy functionals, the basis sets used to expand the Kohn-Sham orbitals, the treatment of core electrons (use and quality of pseudopotentials), and the type of atoms in the system. We are working towards development of fully analytic implementation of density functional theory(ADFT)[7, 8]. The computationally efficient ADFT and efficient use of the available point group symmetry of molecules allow us to optimize large inorganic and carbon fullerenes containing more than two thousand atoms[9, 10].

The ADFT uses analytic atom-centered, localized Gaussian basis sets. These basis sets are used to to ex-

*Electronic address: rzope@alchemy.nrl.navy.mil

[†]Electronic address: dunlap@nrl.navy.mil

pand the molecular (Kohn-Sham) orbitals and the one body effective (Kohn-Sham) potential using variational and robust fitting methodology[11, 12]. The exchange-correlation part of Kohn-Sham potential is obtained using the functional form that is based on Slater's exchange functional[13]. For this reason, the analytic implementation is also called as Slater-Roothaan (SR) method[7]. The SR method allows an arbitrary scaling of the exchange potential around each type of atoms in the heteroatomic systems. These scaling factors can be used to parametrize the SR method. Using a suitable choice of these scaling parameters, accurate total and atomization energies that are comparable to some of the most sophisticated density functional models can be obtained[8, 14, 15]. In the following section we describe the analytic implementation of the density functional model and the details of the SR method.

A. Analytic formulation of the Gàspar-Kohn-Sham-Slater density functional model

In the Hohenberg-Kohn-Sham formulation of the density functional theory[5, 6] the total electronic energy of system containing N electrons and M nuclei is given by

$$E^{HKS}[\rho] = \sum_i^N \langle \phi_i | f_1 | \phi_i \rangle + E_{ee} + E_{xc}[\rho_\uparrow, \rho_\downarrow] \quad (1)$$

where, the first term contains the kinetic energy operator and the nuclear attractive potential due to the M nuclei,

$$f_1 = -\frac{\nabla^2}{2} - \sum_A^M \frac{Z_A}{|\vec{r} - \vec{R}_A|}. \quad (2)$$

The second term in Eq. (1) represents the classical Coulomb interaction energy of electrons while the last term is the exchange-correlation energy that represents contributions that are quantal in origin. The Eq. (1) is an exact expression for the total energy but practical application require approximation to the E_{xc} . Over the years numerous parameterization of different accuracy and complexity have been devised and are available in literature to model E_{xc} . Most of them however

have complex functional form making use of numerical grids necessary in implementations of the DF models. Number of groups have developed numerical integration methods for computation of integrals over the exchange-correlation contributions[16]. Today practically all implementations of the DF models use numerical grids to compute the contribution to the total energy and matrix elements from the exchange-correlation terms. This is true even if analytic basis sets such as Gaussian are used to express KS orbitals. However, it turns out that if one models the E_{xc} according to Gàspar-Kohn-Sham-Slater then the contribution to total energy from this term can also be calculated analytically using the Gaussian basis sets and variational methodology[12, 17, 18].

The Gàspar-Kohn-Sham-Slater (GKS) exchange energy functional is given by

$$E_{xc}[\rho_\uparrow, \rho_\downarrow] = -\frac{9}{8}\alpha\left(\frac{6}{\pi}\right)^{1/3} \int d^3r \left[\rho_\uparrow^{4/3}(\vec{r}) + \rho_\downarrow^{4/3}(\vec{r}) \right]. \quad (3)$$

where, $\alpha = 2/3$ is the Gàspar-Kohn-Sham value and $\alpha = 1$ is the Slater's value. In order to calculate E_{xc} analytically the one-third and two-third powers of the electron density are expanded in Gaussian basis sets:

$$\rho^{1/3}(\vec{r}) \approx \bar{\rho}^{1/3} = \sum_i e_i E_i \quad (4)$$

$$\rho^{2/3}(\vec{r}) \approx \bar{\rho}^{2/3} = \sum_i f_i F_i. \quad (5)$$

Here, $\{E_i\}$ and $\{F_i\}$ are independent Gaussian basis functions, while e_i and f_i are expansion coefficients. The exchange energy is then given by[12, 17, 18]

$$E_{xc} = C_\alpha \left[\frac{4}{3} \langle \rho \bar{\rho}^{1/3} \rangle - \frac{2}{3} \langle \bar{\rho}^{1/3} \bar{\rho}^{1/3} \bar{\rho}^{2/3} \rangle + \frac{1}{3} \langle \bar{\rho}^{2/3} \bar{\rho}^{2/3} \rangle \right], \quad (6)$$

where $C_\alpha = -9\alpha\left(\frac{3}{\pi}\right)^{1/3}$. Thus using four LCGO basis sets (one for orbital expansion and three for the fitting the Kohn-Sham potential) the total energy is calculated analytically.

Similarly, to compute the Coulomb energy,

$$E_{ee} = \langle \rho || \rho \rangle = \frac{1}{2} \int \int \frac{\rho(\vec{r})\rho(\vec{r}')}{|\vec{r} - \vec{r}'|} d^3r d^3r', \quad (7)$$

we use the first robust and variational fitting methodology and express the charge density as a fit to a set of

Gaussian functions,

$$\rho(\vec{r}) \approx \bar{\rho}(\vec{r}) = \sum_i d_i G_i(\vec{r}). \quad (8)$$

Here, $\bar{\rho}(\vec{r})$ is the fitted density, d_i is the expansion coefficient of the charge density Gaussian basis-function G_i . The elimination of the first order error in total energy due to the fit leads to the unique robust expression for the self-Coulomb energy[11]. The LCAO orbital coefficients and the vectors \mathbf{d} , \mathbf{e} , and \mathbf{f} are found by constrained variation. It is easy to obtain contribution from the first term in Eq. (1) in analytic fashion. Thus, in ADFT four sets of Gaussian basis are required: one for KS orbitals, three for the KS effective potential. This methodology was successfully implemented by Werpentski and Cook who demonstrated that noise-free forces and smooth potential energy can be obtained using a *fully analytic* (grid-free) implementation[17, 18].

B. Slater-Roothaan method

While the above analytic implementation is computationally efficient its performance for the atomization of molecules is limited due to the limitation of the functional form adopted. We have tested its performance by computing atomization energies of a set of 56 molecules from the G2 dataset. For $\alpha = 2/3$, the mean absolute error in atomization of 56 molecules is about 16 kcal/mol. This can be improved to 12 kcal/mol by allowing value of α to change[19]. Thus the α in Eq. (6) can be viewed as a scaling parameter that scales exchange potential. The above model then can be modified so that each type of atom in the heteroatomic system has its own value of scaling parameter. This led to the development of the Slater-Roothaan (SR) method[7]. Apart from the advantage that the calculations can be performed in complete analytic fashion, it also allows molecules to dissociate correctly in atomized limit[20]. The exchange energy in

the SR method has following form[7, 15]:

$$\begin{aligned} E^{SR} = & \sum_i \langle \phi_i | f_1 | \phi_i \rangle + 2 \langle \rho | |\bar{\rho} \rangle - \langle \bar{\rho} | |\bar{\rho} \rangle \\ & - \sum_{\sigma=\uparrow,\downarrow} C_x \left[\frac{4}{3} \langle g_B \bar{g}_B^{\frac{1}{3}} \rangle - \frac{2}{3} \langle \bar{g}_B^{\frac{1}{3}} \bar{g}_B^{\frac{1}{3}} \bar{g}_B^{\frac{2}{3}} \rangle \right. \\ & \left. + \frac{1}{3} \langle \bar{g}_B^{\frac{2}{3}} \bar{g}_B^{\frac{2}{3}} \rangle \right]. \end{aligned} \quad (9)$$

Here, $C_x = C_\alpha/\alpha$; the partitioned 3/4 power of the exchange energy density,

$$g_B(\vec{r}) = \sum_{ij} \alpha(i) \alpha(j) D_{ij}^B(\vec{r}), \quad (10)$$

where $D_{ij}^B(\vec{r})$ is the diagonal part of the spin density matrix multiplied by the partitioning function,

$$\alpha(i) = \alpha_i^{3/8} \quad (11)$$

which contains α_i , the α in the X α model for the atom on which the atomic orbital i is centered. The fits to powers of g_σ are obtained variationally from Eq. (9).

I. COMPUTATIONAL DETAILS

As noted earlier the analytic SR method requires four Gaussian basis sets. One for the orbital expansion and others to fit different powers of electron density, which we obtain from literature. We choose Pople's triple- ζ (TZ) 6-311G** basis[21, 22] and the DGauss[24] valence double- ζ (DZ) basis set[25] called DZVP2 for orbitals basis sets. The s -type fitting bases are obtained by scaling and uncontracting the s part of the orbital basis. The scaling factors are 2 for the density, $\frac{2}{3}$ for $\bar{\rho}^{\frac{1}{3}}$ and $\frac{4}{3}$ for $\bar{\rho}^{\frac{2}{3}}$. These scaled bases are used for all s -type fitting bases. Ahlrichs' group has generated a RI-J basis for fitting the charge density of a valence triple- ζ orbital basis set used in the TURBOMOLE program [26]. The non- s parts of Ahlrich's fitting bases are used in combination with the 6-311G** orbital basis sets. We use this combination of basis sets (6-311G**/RIJ) for boron nitride cages and carbon fullerenes. In combination with DZVP2 orbital basis, we use the pd part of the A2 charge density fitting basis. The combination DZVP2/A2 is used for studying aluminum nitride cages. The geometries

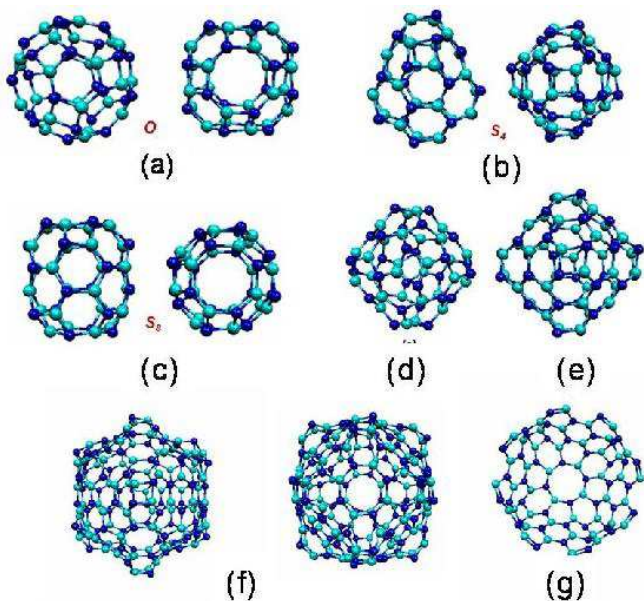


FIG. 1: The optimized BN cages: (a) Two views of the octahedral $B_{24}N_{24}$ cage, (b) Two views of the S_4 $B_{24}N_{24}$ cage, (c) S_8 $B_{24}N_{24}$ cage, (d) $B_{28}N_{28}$ cage of T symmetry, (e) $B_{36}N_{36}$ cage of T_d symmetry, (f) octahedral $B_{96}N_{96}$ cage, and (g) hemispherical cap of (8,8) BN nanotube based on half of $B_{96}N_{96}$.

of molecules were optimized using the Broyden-Fletcher-Goldfarb-Shanno (BFGS) algorithm[27]. The forces on atoms are rapidly computed non-recursively using the 4-j generalized Gaunt coefficients [9, 28]. The atomic energies are obtained in the highest symmetry for which the self-consistent solutions have integral occupation numbers. The atomization energy is computed from the total energy difference of optimized molecule and its constituent atoms.

II. BORON AND ALUMINUM NITRIDE CAGES

The discovery of carbon fullerene C_{60} , followed by discovery of higher fullerenes and carbon nanotubes has led to intense search for hollow cage-like and tube-like structures of other materials. In this search, boron nitride (BN) is probably the second most studied material after carbon. A number of groups have reported observation of BN nanotubes as well as cage like structures[29, 30, 31, 32]. Particular relevant to this article are the series of ex-

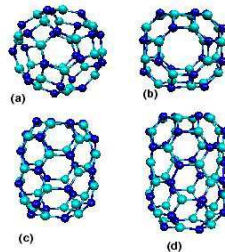


FIG. 2: The optimized structures of capped BN nanotubes. (a) and (b) are two different views of the $B_{24}N_{24}$ cage: (a) along the C_3 axis, (b) along C_4 axis. (c) $B_{28}N_{28}$ (C_{4h}) cage obtained by adding a ring of 8 alternate B and N atoms, (d) tubular $B_{32}N_{32}$ (S_8) cage by inserting two rings of 8 alternate B and N atoms (see text for more details).

TABLE I: The calculated values of binding energy per AlN pair, the energy gap between the highest occupied molecular orbital and the lowest unoccupied molecular orbital, the vertical ionization potential (VIP), the electron affinity, and the energy gap obtained from the ΔSCF calculation for the optimized AlN cages. Last row gives range of values for the same set of BN clusters. All energies are in eV.

	Symmetry	BE	GAP	VIP	VEA	ΔSCF
$Al_{24}N_{24}$	O	10.24	2.97	7.05	1.46	5.59
$Al_{24}N_{24}$	S_4	10.34	2.47	6.84	1.72	5.12
$Al_{24}N_{24}$	S_8	10.34	2.63	6.79	1.58	5.21
$Al_{28}N_{28}$	C_{4h}	10.42	2.74	6.81	1.59	5.22
$Al_{28}N_{28}$	T	10.45	2.67	6.84	1.69	5.15
$Al_{32}N_{32}$	S_8	10.49	2.79	6.77	1.61	5.16
$Al_{36}N_{36}$	T_d	10.54	2.70	6.73	1.76	4.95
$Al_{48}N_{48}$	S_d	11.09	2.81	6.56	1.76	4.8
$Al_{96}N_{96}$	O	10.48	2.18	6.15	2.34	3.8
BN range		15	4-5	7-9	0	7-9

periments by Oku and coworkers in which they detected BN clusters in mass spectrum[29, 32]. These authors have proposed a number of cage like structures for the BN clusters detected in mass spectrum. Here, we report the electronic structure of these cages and their aluminum nitride (AlN) analogues. We note that while of the BN cages has been reported, no cage like structure of AlN have not yet been observed although observations of the AlN nanotubes have been recently noted[33, 34, 35, 36].

The optimized cage structures of BN are given in Fig. 1. Also, given are the symmetries of these cage structures. All these cage structures have been found to be energetically stable with binding energy (BE) of about 14-16 eV per pair of BN. Notable amongst these is the octahedral $B_{24}N_{24}$ cage that was proposed by Oku and coworkers as a candidate structure for one of the most abundant cluster in the mass spectrum. This cage is perfectly round and like in C_{60} fullerene where each carbon atom is equivalent to all other carbon atoms, a pair of BN in this cluster is equivalent to other pairs in the cluster. It is to be noted that the exact analogue of carbon fullerene is not possible for alternate boron nitride cages. The presence of pentagonal rings in carbon fullerenes do not permit full alternation of B and N atoms. Thus even membered rings are necessary to make alternate fullerenes close. The octahedral round $B_{24}N_{24}$ cage contains six square and six octagons. This structure can be used to form caps for (4,4) BN nanotubes[37]. However, unlike C_{60} fullerenes, the round $B_{24}N_{24}$ octahedral cage is not energetically special. The other alternate $B_{24}N_{24}$ cages with symmetry S_4 and S_8 are energetically nearly degenerate with octahedral cage[38]. So it is not clear that which structure is likely to be observed in the experiment.

The C_{4h} $B_{28}N_{28}$ cage [Fig. 2(c)] can be generated from the base $B_{24}N_{24}$ cage by cutting the latter into two halves after orienting it along the C_4 axis, then inserting a ring of eight alternate B and N atoms perpendicular to the axis, i.e. horizontally, and then rotating the top half by an eighth of a revolution. The resultant cage contains 8 inequivalent atoms and has C_{4h} symmetry. If two rings of four alternate BN pair are inserted instead of one then

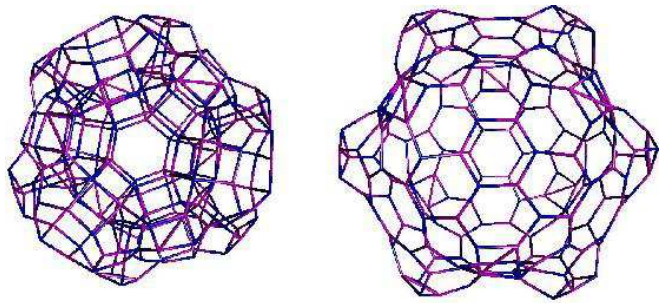


FIG. 3: Optimized octahedral $Al_{96}N_{96}$ cages: (a) Two shell onion-like octahedral cage with $Al_{24}N_{24}$ cage at its interior $Al_{96}N_{96}$ -I, (b) Fullerene-like cage $Al_{96}N_{96}$ -II.

the resultant $B_{32}N_{32}$ cage is a tubular structure with S_8 symmetry. The binding energy systematically increases by going from $B_{24}N_{24}$ to the $B_{28}N_{28}$ cage (0.26 eV per BN pair) and from $B_{28}N_{28}$ to $B_{32}N_{32}$ cage (0.06 eV/BN pair). The successive additions of alternate BN rings energetically stabilizes the BN tubular cages and results in (4,4) BN nanotube with round caps that are based on octahedral $B_{24}N_{24}$ cage. Note that same (4,4) tube can also be generated by starting with S_8 $B_{24}N_{24}$ cage structure. The hemispherical caps of (4,4) tube based on octahedral $B_{24}N_{24}$ that we have proposed have also been observed in a molecular dynamics study of the growth mechanism of BN nanotubes[39].

The $B_{24}N_{24}$ can be enlarged by adding hexagons. This leads to another round cage $B_{96}N_{96}$ of octahedral symmetry. The optimized $B_{96}N_{96}$ cage is shown in Fig. 1 (f). Energetically the $B_{96}N_{96}$ cage is more stable than the $B_{24}N_{24}$ cage. It is clearly different, from $B_{24}N_{24}$, in that while being mostly round, its twelve squares stick out significantly, like the detonators of a sea mine. Its halves can form a round cap for the (8,8) BN nanotube (See Fig. 1 (g)).

We have reoptimized the BN cages by replacing boron by aluminum. We would like to point out that unlike BN cages which are experimentally observed, the AlN cages studied here are predictions. The optimized cage structures in AlN are similar to those of BN except that they are larger in size due to the larger AlN bond distance than that of BN. The exception to this trend is the $Al_{96}N_{96}$

TABLE II: The median nearest-neighbor bond distance, mean radius, radial standard deviation, all in Angstroms, for the fullerenes of this work computed using $\epsilon = 0.684667$. The right-most column gives the atomization energy per atom (AE), in electron volts, that we compute using $\epsilon = 0.64190$.

Fullerene	Median bond distance	Mean radius	AE
C ₆₀	1.4244	3.5481	-7.140
C ₂₄₀	1.4306	7.0728	-7.373
C ₅₄₀	1.4264	10.5528	-7.431
C ₉₆₀	1.4249	14.0342	-7.459
C ₁₅₀₀	1.4244	17.5225	-7.474
C ₂₁₆₀	1.4241	21.0137	-7.484

cluster (See Fig. 3). The optimization of Al₉₆N₉₆ structure starting from B₉₆N₉₆ cluster results in formation of double shell onion like structure. This onion cluster has Al₂₄N₂₄ cage at its core[40]. On the other hand, if one scales the B₃₆N₃₆ to account for larger AlN bond length and then replace B by Al and optimize then one does get fullerene like hollow cage with squares sticking out. This cage will be referred to as Al₉₆N₉₆ -II. We find that all AlN cages are energetically stable with binding energy of about 10-11 eV per pair of AlN. However, the binding energy of AlN cages is less than BN cages, which have binding energy of 14-16 eV per BN pair. Similarly, the ionization potential (IP) and the energy gap between the energy eigenvalues of highest occupied molecular orbital (HOMO) and the lowest unoccupied molecular orbital is smaller in AlN cages. The vertical IP of BN cages is in the range 7-9 eV while it is about 6-7 eV in AlN cages. Due to the large HOMO-LUMO gap in the BN cages, the BN cages do not like to bind an extra electron. Consequently, the electron affinity of boron nitride cages is practically zero within our model. The AlN cages have electron affinity of about 1-2 eV. We have summarized the electronic structure data of AlN cages in Table I. In the last row of the same table contains the range of values for the BN cages. The HOMO-LUMO gap calculated by the so called ΔSCF method in which the first ionization potential is subtracted from the first electron affinity is given in the last row of the table.

Fully optimized fullerenes by analytic DFT (all electron calc. 6311G** basis)

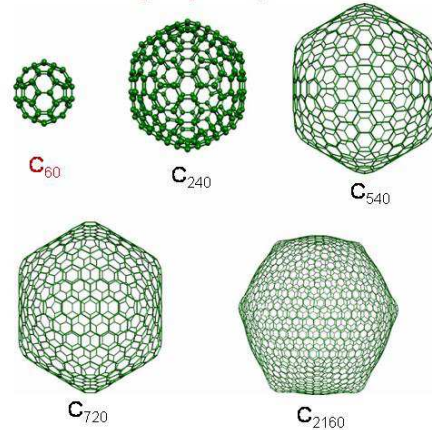


FIG. 4: Fully optimized structures carbon fullerenes (Basis set: 6-311G**/Ahlich) (see text for more details).

III. CARBON FULLERENES

Carbon fullerenes structures larger than 100 atoms have been studied by several groups[41, 42, 43]. Most of these studies have used semiempirical models or tight binding methods or the Hartree-Fock theory plus minimal basis sets. Except for very recent calculation[44] on C₂₄₀, fullerenes have not been studied using reasonable quality basis sets[45]. This is principally because of large computational cost. We have used computationally efficient ADFT described above to optimize geometries of several carbon fullerenes from C₆₀ to C₂₁₆₀ using large polarized Gaussian basis sets of triple zeta quality (6-311G**)[10]. The ADFT code developed in our group exploits the icosahedral symmetry of these fullerenes in an efficient manner. Therefore, very large calculation on C₂₁₆₀ with about 39000 orbital basis functions, is still doable with modest computation resources. In order to get accurate geometries of larger fullerenes, we parametrize the ADFT to get the exact geometry of C₆₀. This is accomplished by minimizing the mean square deviation between the experimental and predicted bond lengths of C₆₀. This is possible without much difficulty as optimization of C₆₀ using ADFT takes less than 5 minutes on single processor Linux box (Intel(R) XEON(TM) CPU 2.20GHz with 2Gigabytes of Random Access Memory). The exact ge-

ometry of C_{60} can be obtained for $\alpha = 0.684667$. We use this value of α for optimizing larger carbon fullerenes and hope that this will give accurate estimates of their geometries. The C_{960} fullerene can be optimized on single processor in 5 days. The C_{2160} optimization was performed on Linux cluster using 48 processors and took about 5 days. The median bond distance of optimized carbon fullerenes is given in Table II and optimized structures are shown in Fig. 4. We also made an attempt to get accurate atomization energies using the optimized geometries of fullerenes. For this purpose we reparametrize ADFT to get the exact binding energy of C_{60} fullerene and use the α value thus determined to compute the atomization energies of larger fullerenes. These values are also given in Table II. However, such a procedure fails in that the atomization energy of C_{240} is already lower than that of graphite. Thus, to get accurate estimate of atomization energy we need to go beyond the functional form that we have chosen in parameterizing the ADFT.

Work is progress in our laboratory in this direction.

IV. CONCLUSION

We have presented fully analytic implementation of density functional theory (ADFT). It uses analytic Gaussian basis sets to variationally express the Kohn-Sham molecular orbitals, electron density and the one body effective potential of the density functional theory. The resultant formulation is computationally very efficient and allow for calculations on relatively large systems. It permits use of atomic number dependent potential by means of Slater's exchange parameters. Using the ADFT code, which efficiently uses the full point group symmetry of the molecule, we have optimized large inorganic fullerene-like cages and carbon fullerenes containing more than two thousand atoms.

-
- [1] See, for example, other contributions from this volume.
 - [2] A. D. Bacon and M. C. Zerner, *Theo. Chim. Acta* **53**, 21 (1979); W. P. Anderson, W. D. Edwards, and M. C. Zerner, *Inorganic Chem.* **25**, 2728 (1986).
 - [3] J. J. P. Stewart, *J. Comp. Chem.* **10**, 209 (1989); J. J. P. Stewart, *J. Comp. Chem.* **10**, 221 (1989).
 - [4] O.K. Andersen and O. Jepsen, *Phys. Rev. Lett.* **53**, 2571 (1984); R.E. Cohen, M.J. Mehl, and D.A. Papaconstantopoulos, *Phys. Rev. B* **50**, 14 694 (1994); M. Menon and J. Connolly, *Phys. Rev. B* **50**, 8903 (1994).
 - [5] P. Hohenberg and W. Kohn, *Phys. Rev.* **136**, B864 (1964).
 - [6] W. Kohn and L. J. Sham, *Phys. Rev.* **140** A1133 (1965).
 - [7] B. I. Dunlap, *J. Phys. Chem.* **107** 10082 (2003);
 - [8] R. R. Zope and B. I. Dunlap, *J. Chem. Theory. Comput.* **1**, 1193 (2005).
 - [9] B. I. Dunlap, *Computer Phys. Comm.* **165**, 18 (2005).
 - [10] B. I. Dunlap and R. R. Zope, *Chem. Phys. Lett.*(in press); cond-mat/0603225
 - [11] B. I. Dunlap, J. W. D. Connolly, and J. R. Sabin, *J. Chem. Phys.* **71**, 3396; 4993 (1979).
 - [12] B. I. Dunlap and N. Rösch, *J. Chim. Phys.* **86**, 671 (1989).
 - [13] J. C. Slater, *Phys. Rev.* **81**, 385 (1951).
 - [14] R. R. Zope and B. I. Dunlap, *Phys. Rev. B* **71**, 193104 (2005).
 - [15] R. R. Zope and B. I. Dunlap, *J. Chem. Phys.* **124**, 044107 (2006).
 - [16] M. R. Pederson and K. A. Jackson, *Phys. Rev. B* **41**, 7453 (1990); K. A. Jackson and M. R. Pederson, *Phys. Rev. B* **42**, 32763281 (1990); P.M.W. Gill, B. G. Johnson, and J. A. Pople, *Chem. Phys. Lett.* **209**, 506 (1993); O. Treutter and R. Ahlrichs, *J. Chem. Phys.* **102**, 346 (1995).
 - [17] K. S. Werpetinski and M. Cook, *Phys. Rev. A* **52**, 3397 (1995).
 - [18] K. S. Werpetinski and M. Cook, *J. Chem. Phys.* **106**, 7124 (1997).
 - [19] R. R. Zope and B. I. Dunlap, *Chem. Phys. Lett.* **399**, 417 (2004).
 - [20] J. C. Slater, *J. Chem. Phys.* **57**, 2389 (1972).
 - [21] R. Krishnan, J. S. Binkley, R. Seeger, and J. A. Pople, *J. Chem. Phys.* **72**, 650, (1980).
 - [22] A. D. McLean, G. S. J. Chandler, *J. Chem. Phys.* **72**, 5639 (1980).

- [23] G. Broyden, J. of the Inst. for Math. and Applications, **6** 222 (1970).
- [24] J. Andzelm, E. Wimmer, J. Phys. B, 172, 307 (1991); J. Chem. Phys. **96**, 1280 (1992).
- [25] N. Godbout, D. R. Salahub, J. Andzelm, E. Wimmer, Can. J. Chem. **70**, 560 (1992).
- [26] K. Eichkorn, F. Weigend, O. Treutler, and R. Ahlrichs, Theor. Chem. Acc. **97**, 119 (1997).
- [27] Press W. H.; Flannery B. P.; Teukolsky S. A.; Vetterling W. T., *Numerical Recipes The Art of Scientific Computing* (Cambridge University Press: Cambridge, England, 1986) p 309.
- [28] B. I. Dunlap, Phys. Rev. A **66**, 032502 (2002).
- [29] T. Oku, A. Nishiwaki, I. Narita, and M. Gonda, Chem. Phys. Lett. **380**, 620 (2003).
- [30] O. Stephan, Y. Bando, A. Loiseau, F. Willamie, N. Shramchenko, T. Tamiya, and
- [31] D. Goldberg, Y. Bando, O. Ste'pahan, and K. Kurashima, Appl. Phys. Lett. **73**, 2441 (1998).
- [32] T. Oku, T. Hirano, M. Kuno, T. Kusunose, K. Nihara, and K. Suanuma, Mater. Sci. and Engg. **B74**, 206 (2000).
- [33] V. N. Tondare, C. Balasubramanian, S. V. Shende, D. S. Joag, V. P. Godbole, and S. V. Bhoraskar, App. Phys. Lett. **80**, 4813 (2002).
- [34] C. Balasubramanian, S. Bellucci, P. Castrucci, M. De Crescenzi, and S. V. Bhoraskar, Chem. Phys. Lett. **383**, 188 (2004).
- [35] C. Balasubramanian, V. P. Godbole, V. K. Rohatgi, A. K. Das and S. V. Bhoraskar, Nanotechnology **15**, 370 (2004).
- [36] Q. Wu, Z. Hu, X. Wang, Y. Lu, X. Chen, H. Xu, and Y. Chen, J. Amer. Chem. Soc. **125**, 10176 (2003).
- [37] R. R. Zope and B. I. Dunlap, Chem. Phys. Lett. **386**, 403 (2004).
- [38] R. R. Zope, T. Baruah, M. R. Pederson, and B. I. Dunlap, Chem. Phys. Lett. **393**, 300 (2004).
- [39] X. Blase, A. De Vita, J.-C. Charlier, and R. Car, Phys. Rev. Lett. **80**, 1666 (1998).
- [40] R. R. Zope and B. I. Dunlap, Phys. Rev. B **72**, 045439 (2005).
- [41] B. I. Dunlap, D. W. Brenner, J. W. Mintmire, R. C. Mowery, and C. T. White, J. Phys. Chem. **95**, 8737 (1991).
- [42] G. E. Scuseria, Science **271**, 942 (1996).
- [43] S. Itoh, P. Ordejón, D. A. Drabold, and R. M. Martin, Phys. Rev. B **53**, 2132 (1996).
- [44] B. Geudtner, F. Janetzko, AM Koster, a Vela, P Calaminici, J. Comp. Chem. **27**, 483 (2006).
- [45] G. E. Scuseria, Chem. Phys. Lett. **243**, 193 (1995).